

Electronic Supplementary Material

NO Reduction with CO over CuO_x/CeO₂ Nanocomposites: Influence of Oxygen Vacancies and their Role in the Reaction Mechanism

*Quanquan Shi,^{a,†} Yuhang Wang,^{b,†} Song Guo,^b Zhong-Kang Han,^{*c} Na Ta^b and Gao Li,^{*b}*

Alfons Baiker^d

^a College of Science, College of Material Science and Art Design, Inner Mongolia Agricultural University, Hohhot 010018, China

^b State Key Laboratory of Catalysis, Dalian Institute of Chemical Physics, Chinese Academy of Sciences, Dalian 116023, China.

^c Center for Energy Science and Technology, Skolkovo Institute of Science and Technology, Skolkovo Innovation Center, Moscow, 143026, Russia

^d Department of Chemistry and Applied Biosciences, Institute for Chemical and Bioengineering, ETH Zurich, Hönggerberg, HCI, CH-8093 Zurich, Switzerland

Raman Spectroscopy

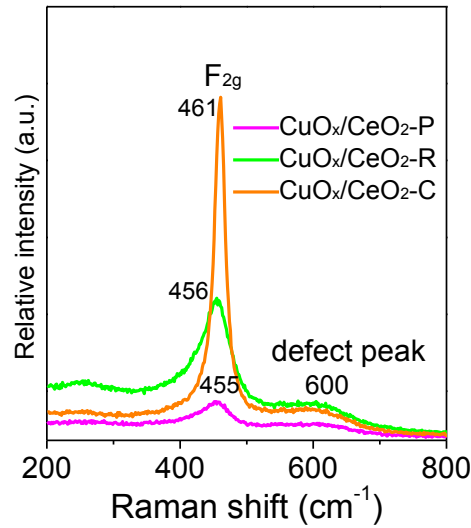


Fig. S-1. Raman spectra of $\text{CuO}_x/\text{CeO}_2$ nanocomposites. The sharp peaks at 455-461 cm^{-1} and the broad ones at $\sim 610 \text{ cm}^{-1}$ are assigned to be the F_{2g} Raman-active mode and the defects in CeO_2 shifts. The F_{2g} shift broadens in $\text{CuO}_x/\text{CeO}_2$ -nanorod samples, indicating the bigger particle size of CeO_2 -nanorods¹, which matches well with the TEM observation (Table 1).

Using the spatial correlation model to calculate the concentration of oxygen vacancy defects

Raman can be used to calculate the relative quantities of oxygen vacancy defects in ceria based on the strong F_{2g} peak and the defect peak using a special correlation model.² First, the halfwidth of the F_{2g} peak (Γ) is related to the crystallite grain size (d_g) through the following correlation:

$$\Gamma(\text{cm}^{-1}) = 5 + 51.8/d_g(\text{nm}) \quad (1)$$

Next, the average distance between two lattice defects (L , nm) is can be estimated as:

$$L(\text{nm}) = \sqrt[3]{\left(\frac{\alpha}{2d_g}\right)^2 + [(d_g - 2\alpha)^2 + 4d_g^2\alpha]} \quad (2)$$

where α is the radius of a CeO_2 molecule (0.34 nm).

The concentration of defects on the surface (N , cm^{-3}) (listed in Table S3) is calculated according to:

$$N = \frac{3}{4\pi L^3} \quad (3)$$

These data are depicted in Table 1.

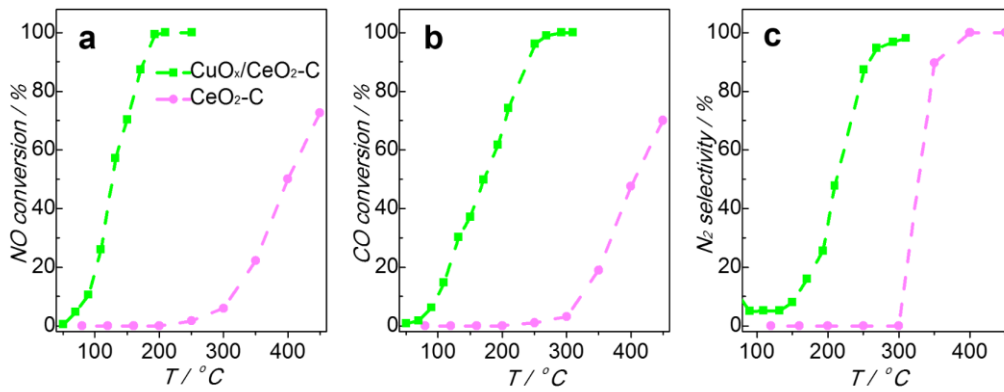


Fig. S-2. Catalytic performances, including (a) CO conversion, (b) NO conversion, and (c) N₂ selectivity, over the CuO_x/CeO₂-C catalysts and CeO₂-C support in the NO reduction with CO as a function of temperature. Reaction conditions: 50 mg catalysts, GHSV = 36,000 mL g⁻¹ h⁻¹, 1 vol% NO and 1 vol% CO in argon balance. The introduction of CuO_x species onto the ceria supports remarkably improved the catalytic performance in the NO reduction with CO.

**Comparison of calculated CO consumptions and detected CO consumptions:
Confirmation of relation between NO and CO balances**

The NO reduction by CO contains two main reactions steps: (5) and (6):



The calculated CO consumption ($X_{\text{CO-calc.}}$) was derived based on the online detected NO conversion and the N₂ selectivity (S_{N_2}) according to:

$$X_{\text{CO-calc.}} = 0.5 * X_{\text{NO}} * (1 + S_{\text{N}_2}) \quad (7)$$

where, X_{NO} represents the NO conversion determined by online GC analyses.

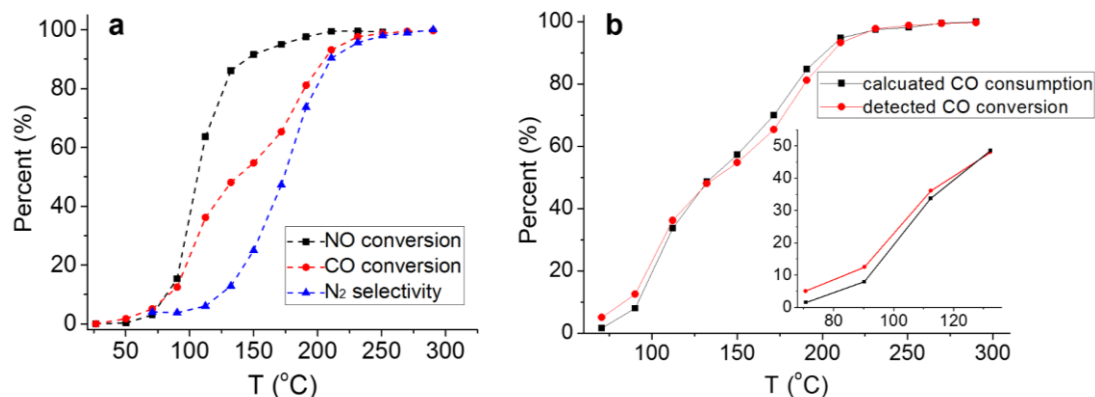


Fig. S-3. (a) Catalytic performance of the CuO_x/CeO₂-R catalyst in the NO reduction by CO. (b) Comparison of the calculated CO consumption (Eq. 7) and the detected CO conversion; inset: the zoom-in of reactivity at 70-130 °C.

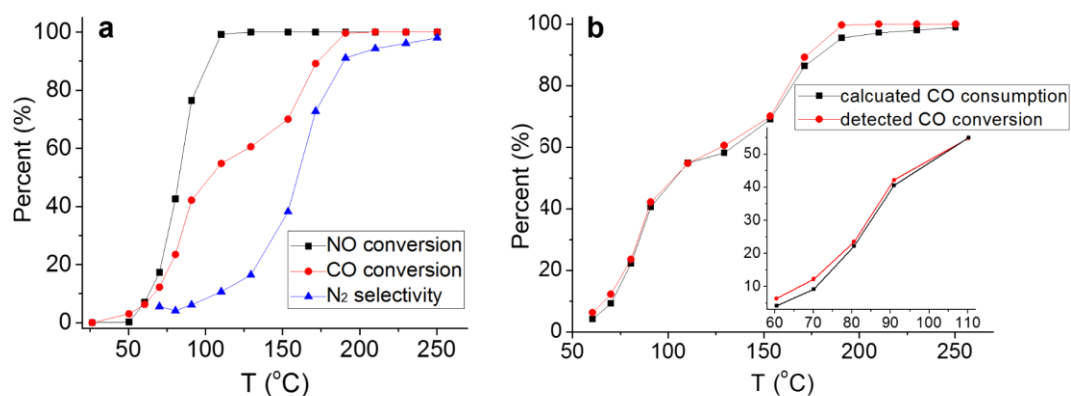


Fig. S-4. (a) Catalytic performance of the CuO_x/CeO₂-P catalyst in the NO reduction by CO. (b) Comparison of the calculated CO consumption (Eq. 7) and the detected CO conversion; inset: the zoom-in of reactivity at 60-115 °C.

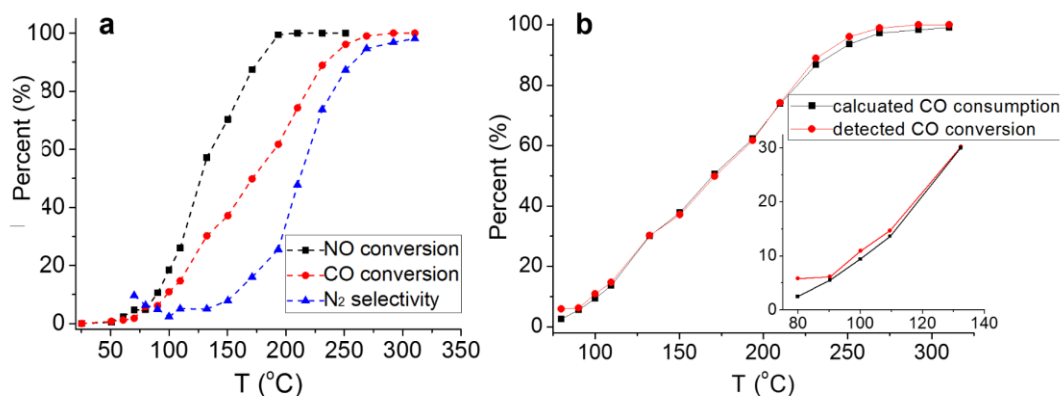


Fig. S-5. (a) Catalytic performance of the CuO_x/CeO₂-C catalyst in the NO reduction by CO. (b) Comparison of the calculated CO consumption (Eq. 7) and the detected CO conversion; inset: the zoom-in of reactivity at 80-130 °C.

Nitrogen adsorption-desorption isotherms of the $\text{CuO}_x\text{-CeO}_2$ catalysts

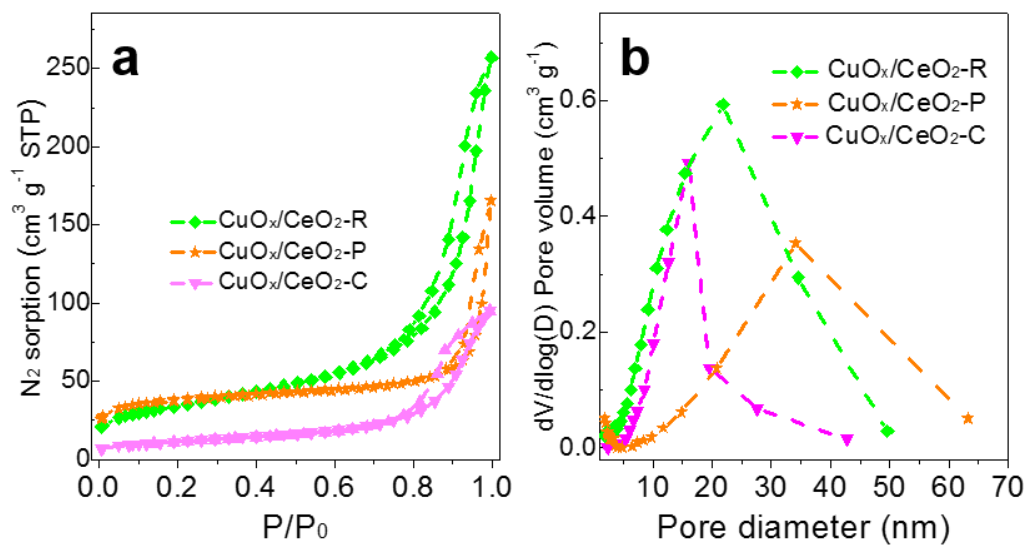


Fig. S-6. (a) N_2 -adsorption-desorption isotherms of the $\text{CuO}_x/\text{CeO}_2$ catalysts, and (b) corresponding pore size distributions determined by the BJH method.

Long-term behavior of CuO_x-CeO₂-R catalyst in NO reduction with CO

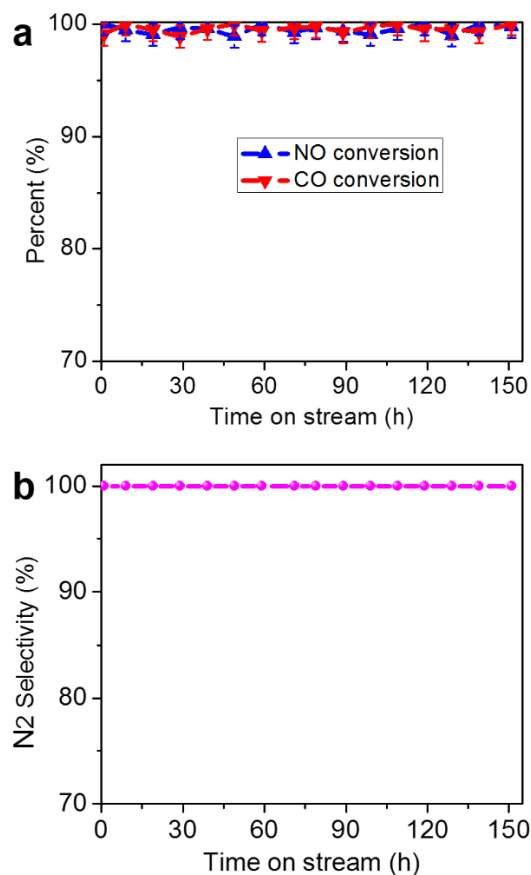


Fig. S-7. Stability test of the CuO_x/CeO₂-P catalyst carried out at 250 °C over 150 h: (a) CO and NO conversions, and (b) N₂ selectivity. Reaction conditions: 50 mg catalysts, GHSV = 36,000 mL g⁻¹ h⁻¹, 1 vol% NO and 1 vol% CO with argon balance.

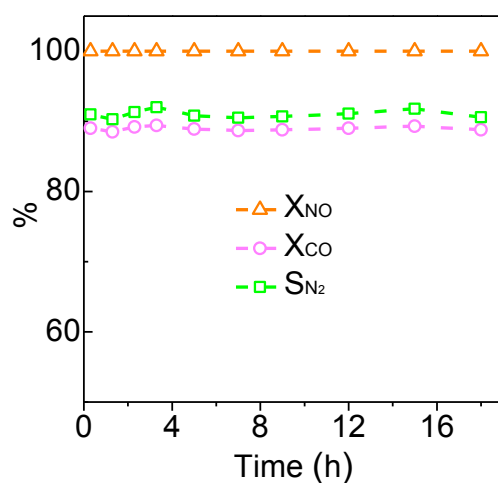


Fig. S-8. Stability test of the CuO_x/CeO₂-P catalyst carried out at 170 °C over 18 h. Reaction conditions: 50 mg catalysts, GHSV = 36,000 mL g⁻¹ h⁻¹, 1 vol% NO and 1 vol% CO with argon balance.

EPR investigation of oxygen vacancy defects

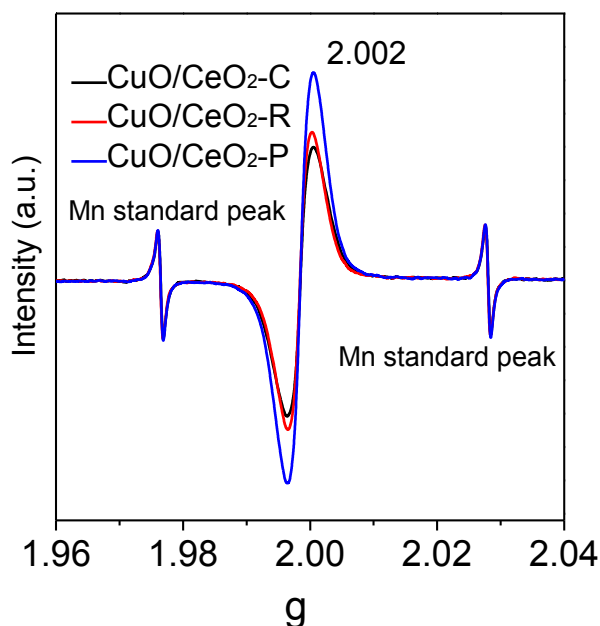


Fig. S-9. EPR spectra of the CuO_x/CeO₂ samples using 2,2,6,6-tetramethylpiperidine-nitrogen-oxide (TEMPO) as the standard sample and Mn^{II} as the reference sample.

Table S1. Concentrations of surface oxygen vacancies in CuO_x/CeO₂ with different morphologies determined by different methods

Sample	O _v /O _{total} ^a	Conc. of O _v (10 ⁻¹² spin mg ⁻¹) ^b	O _v conc. (10 ²¹ cm ⁻³) ^c
CuO _x /CeO ₂ -C	0.18	2.6	2.5
CuO _x /CeO ₂ -R	0.26	3.2	5.3
CuO _x /CeO ₂ -P	0.32	5.8	6.1

Notes: ^a determined by XPS analyses (Figure 4). ^b determined by the EPR measurements (Figure S7). ^c determined by the Raman spectroscopy using spatial correlation model (Figure S1). O_v = oxygen vacancy, Conc. = concentration.

As shown in Table 2, the concentration of the surface oxygen vacancies, determined by all methods, XPS, EPR, and Raman spectroscopy, used in this work, follows the order of CuO_x/CeO₂-P > CuO_x/CeO₂-R > CuO_x/CeO₂-C.

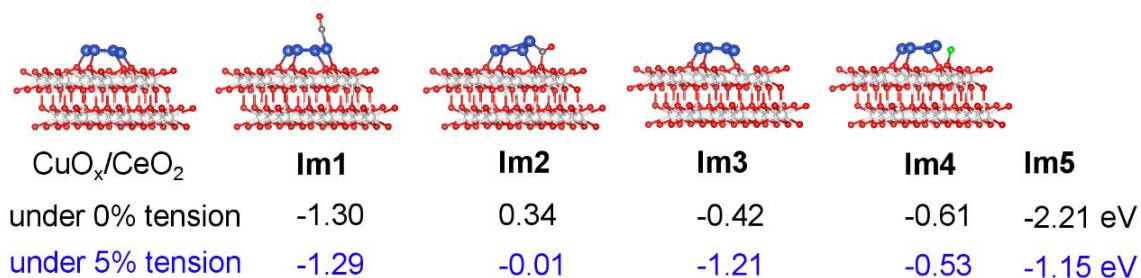


Fig. S-10. The reaction coordinates of the NO reduction with CO over the other structural model, where all the Cu atoms are in contact with the surface lattice oxygen of ceria. The values from left to right are the CO-adsorption energy (**Im1**), reaction energy from CO with O_L to yield -CO₂ complex (**Im2**), CO₂-desorption energy (**Im3**), NO-adsorption energy (**Im4**), and N₂-desorption energy (**Im5**) under 0% tension (in black) and 5% tension (in blue). Color code: Ce atoms, white; O atoms, red; Cu atoms, blue.

References

1. W. H. Weber, K.C. Hass, J.R. McBride, Raman study of CeO₂: Second-order scattering, lattice dynamics, and particle-size effects, *Phys. Rev. B* **1993**, 48, 178-185.
2. L. Saveriede, S. L. Nauert, C. A. Roberts, J. M. Notestein, The effect of support morphology on Co_xO_y/CeO₂ catalysts for the reduction of NO by CO. *J. Catal.* **2018**, 366, 150-158.